

Development of an Electrospray Fragmentation Model for Kinetic Plume Modeling

IEPC-2019-830

*Presented at the 36th International Electric Propulsion Conference
University of Vienna, Austria
September 15-20, 2019*

Elaine M. Petro*, Catherine E. Miller†, Joseph Schmidt‡ and Paulo C. Lozano§
Massachusetts Institute of Technology, Cambridge, MA, 02138, USA

A physics-based electrospray plume model that incorporates processes specific to ionic liquid ion sources is under development. Recent progress in experimental characterization of the fragmentation of heavy ion species is summarized. The experimentally verified model for fragmentation is incorporated into a particle-in-cell model of electrospray plume evolution. Tracking fragmentation processes in coordination with charged particle extraction and acceleration is critical for accurately predicting plume divergence, energy distribution, and particle trajectories. Outputs of this model will serve as inputs into follow-on models of array-level and spacecraft-level plume interactions.

Nomenclature

A	= constant rate coefficient
E	= electric field
E_a	= activation energy
ϵ_0	= permittivity of free space
f_f	= current fraction of fragmented dimers
f_o	= current fraction of monomers
F	= thrust
f_f	= current fraction of fragmented dimers
k	= Boltzmann constant
K	= fragmentation rate
m	= mass
η_p	= polydispersive efficiency
τ	= fragmentation time constant
T	= ion temperature
q	= charge
V_i	= injection potential
ζ	= mass ratio of monomer to dimer

*Post Doctoral Associate, Department of Aeronautics and Astronautics, epetro@mit.edu.

†Research Associate, Department of Aeronautics and Astronautics, millerce@mit.edu.

‡Visiting Undergraduate Research Assistant, Department of Aeronautics and Astronautics, joeschm@mit.edu

§M. Alemán-Velasco Professor, Department of Aeronautics and Astronautics, plozano@mit.edu.

I. Motivation

Electrospray thrusters are a promising form of micropropulsion with the ability to provide primary propulsion for small satellites and precision control for larger platforms.¹ There is growing demand for flight implementations which motivates the desire to understand the coupled effects between thruster plume particles and the host spacecraft. The ability to predict these effects will lead to better understanding of on-orbit thruster performance and the ability to mitigate degradation of sensitive spacecraft surfaces. While models with this objective have been developed for other electric propulsion devices,² an appropriate source model must be developed to perform similar studies with electrospray thrusters.

Electrospray thrusters differ from plasma-based systems in two key ways, motivating the development of a unique source model. First, the ions comprising electrospray plumes are molecular species with complex internal degrees of freedom. For example, the post-emission fragmentation of heavy ion clusters impacts beam composition, ion energy distribution, and thereby thruster performance.³ Capturing these molecular processes is essential for determining interactions with the host spacecraft, from contamination and erosion to local and global charging.⁴ Second, electrospray ion generation and acceleration are coupled through the extraction process and occur over a volume characterized by a size that is orders of magnitude smaller than in conventional plasma thrusters ($<100 \mu\text{m}$, down to a few nm in the emission region). It is critical to resolve ion trajectories within and in the near-vicinity of this region to accurately capture the plume evolution. Resolution of this region is also essential for tracking ion backscatter and resulting grid erosion.

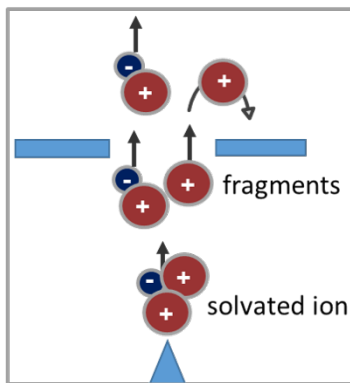


Figure 1: Diagram depicting fragmentation and current return within the local volume of an electrospray ion source.

Thus a proper model of electrospray ion emission will integrate conditions influencing emission from individual sites and propagate the particle trajectories throughout the extraction and acceleration region. The predicted plume characteristics (composition, velocity distribution, fragmentation rates) will eventually be used to generate descriptions of an electrospray particle source in a larger simulation volume that includes spacecraft-level interactions.

In this work, a model for tracking the breakup of heavy species is developed and implemented into a particle-in-cell (PIC) routine for an electrospray source. First, the model for solvated ion fragmentation is discussed and empirically derived results are presented. Next, an algorithm for incorporating the fragmentation process into the PIC routine is presented, along with preliminary simulation results. This work represents the first steps in developing a comprehensive simulation platform for electrospray plumes.

II. Fragmentation: Performance Effects and Characterization

A. Effects of Fragmentation on Thruster Performance

Ion electrospray thrusters produce ion beams containing a wide diversity of ion species including single ions and ion clusters. In this work, we refer to single ions as monomers. The smallest ion cluster is referred to as a dimer, which is a single ion attached to a cation-anion pair, or neutral cluster. The next largest cluster is a trimer, which is a single ion attached to two cation-anion pairs. Even larger ion clusters, such as tetramers and pentamers, are sometimes observed in small quantities.⁵ Ion electrospray thruster beams

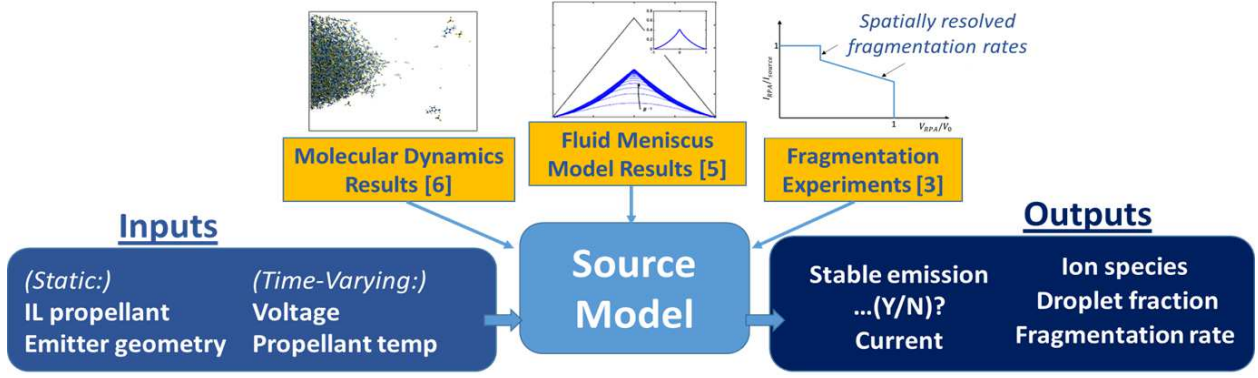


Figure 2: Diagram depicting critical input parameters which influence source operation and output parameters captured in the source model.

typically consist of monomers, dimers, and trimers. The relative amounts of each species depends on the ionic liquid as well as on the thruster operating conditions.⁵ The presence of single ions and ion clusters decreases the overall performance of ion electrospray thrusters.⁶ This is due to the fact that ion species are accelerated to different final velocities according to their respective masses, which increases the polydispersity of the ion beam and decreases the efficiency and specific impulse.⁶

The thruster performance is also affected by the fragmentation of ion clusters. When ion clusters break up during the acceleration phase, a smaller ion, referred to as the broken ion, and a neutral cluster are produced. The broken ion is accelerated to a final kinetic energy, always less than the source potential, which depends on the location where the parent ion broke up. Since the ion clusters can break apart anywhere along their journey from the emitter tip to the extractor, this means that broken ions will be accelerated to a spread in final kinetic energies and thus a spread in final velocities. Additionally the neutral clusters cannot be accelerated by the electric field, so they exit the thruster low velocities that depend on where the parent ions broke up. These two effects increase the polydispersity of the beam and decrease the thruster performance.⁷ The polydisperse efficiency, η_p , can be modeled using the following equation:⁷

$$\eta_p = \frac{\left(1 + (\sqrt{\xi} - 1)f_0 + \frac{1}{3}f_f \left(2\sqrt{\xi} \frac{1-\sqrt{\xi}}{1-\xi} - 1\right)\right)^2}{1 + (\xi - 1)f_0} \quad (1)$$

where ξ is the mass ratio of monomer to dimer, f_0 is the current fraction of monomers, and f_f is the current fraction of dimers that break up within the acceleration region. The effect of fragmentation on thrust, F , can be estimated using the following expression:^{7,8}

$$\frac{F}{F_{ideal}} = 1 - \frac{\frac{1}{3}f_f \left(\frac{1-\sqrt{\xi}}{1+\sqrt{\xi}}\right)}{1 + (\sqrt{\xi} - 1)f_0} \quad (2)$$

where F_{ideal} is the thrust for a beam without fragmentation. The ratio of F/F_{ideal} is also equivalent to the change in specific impulse, $I_{sp}/I_{sp,ideal}$. Note that in deriving these expressions, it was assumed that the amount of dimer fragmentation occurs uniformly with respect to the acceleration potential.⁷ The effect of fragmentation on thruster performance, modeled by Equations 1-2, is represented graphically in Figure 3. In addition to affecting thruster performance, fragmentation is a critical process for spacecraft neutralization,⁴ which is why accurate modeling of fragmentation is essential.

B. Fragmentation Characterization and Modeling

Recent experiments by Miller have shown that fragmentation, on average across the beam, can be modeled as an activated process.⁸ In the region outside the thruster, called the field-free region, the fragmentation of dimers was experimentally observed to follow a constant-rate equation.⁸ This was achieved by measuring

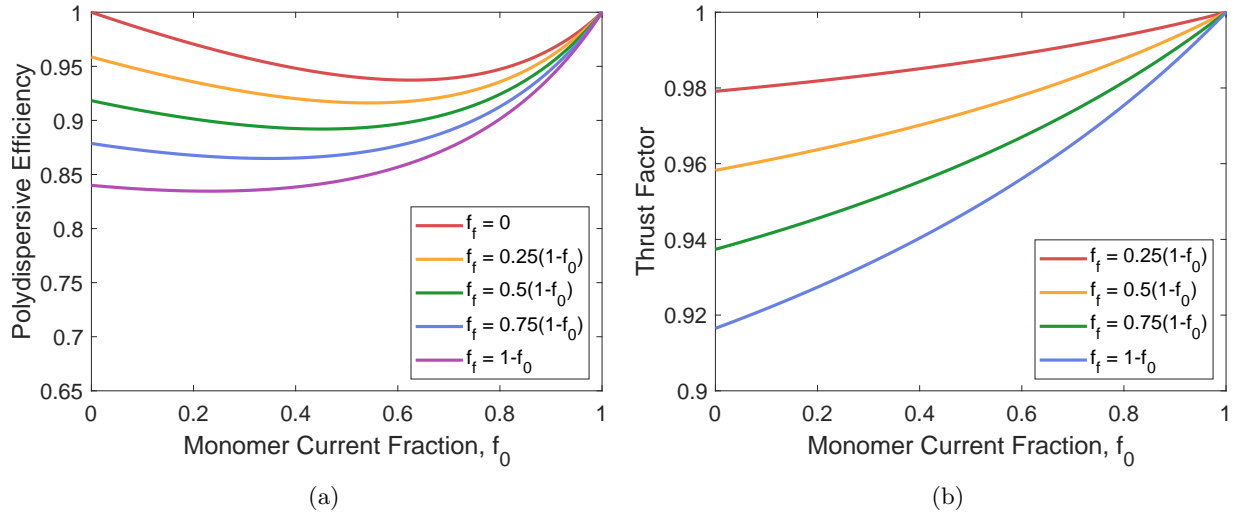


Figure 3: Polydispersive efficiency and thrust reduction factor for positive EMI-BF₄ ILIS beams with dimer fragmentation.⁸

the amount of dimer fragmentation in the field-free region using a full-beam, spherical geometry retarding potential analyzer (RPA). The amount of dimer fragmentation was measured as a function of the distance between the single-emitter electro spray thruster and the RPA. The data were fitted using a constant rate equation:⁸

$$f_f = f_{di,0} \left(1 - e^{-t/\tau} \right) \quad (3)$$

where f_f is the current fraction of dimers that fragment in the field-free region, $f_{di,0}$ is the current fraction of dimers that enter the field-free region, t is the time dimers spend in the field-free region before detection by the RPA, and τ is the inverse of the mean fragmentation rate, K , and is referred to as the mean lifetime.⁸ Figure 4 shows the fitted data for EMI-BF₄ dimer fragmentation in the field-free region. In this example, the

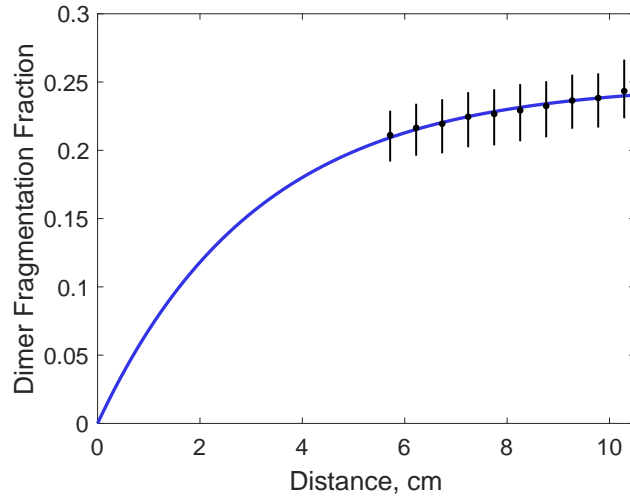


Figure 4: Dimer fragmentation curve for a single-emitter EMI-BF₄ electro spray thruster operating at $T = 30^\circ\text{C}$, $V = 859\text{V}$, and $I = 324\text{nA}$.⁸

mean lifetime of positive EMI-BF₄ dimers is $1.49 \mu\text{s}$. Note that to calculate the mean lifetime, the distance between the source and the RPA is converted to the time the dimer spent traveling to the RPA using the dimer velocity. Several ionic liquids were tested and, on average, the dimer mean lifetimes ranged from 1-6 microseconds.⁸

Miller also studied ion cluster fragmentation in the acceleration region, which is the space between the emitter tips and extractor plate. The presence of the electric field in the acceleration region enhances the rates of fragmentation. This is particularly true of the region close to the emitter tip, where the electric field is strongest. Miller studied a variety of models to describe the effect of an external electric field on the fragmentation rates. For example, the fragmentation rate, K , in the field-free region can be described using the following expression for an activated process:

$$K = A \exp \left[-\frac{E_a}{kT} \right] \quad (4)$$

where A is the constant rate coefficient, E_a is the activation energy, k is Boltzmann's constant, and T is the initial internal temperature of the ion cluster.⁸ An external electric field decreases the energy barrier for fragmentation because it separates oppositely charged ions. Using the Iribarne and Thomson model for ion evaporation,⁹ the fragmentation rate of ion clusters in the presence of an external electric field can be modeled using the following expression:

$$K = A \exp \left[-\frac{1}{kT} \left(E_a - \sqrt{\frac{q^3 E}{4\pi\epsilon_0}} \right) \right] \quad (5)$$

where q is the ion charge, E is the magnitude of the electric field, and ϵ_0 is the permittivity of free space.⁸ The results of this model are qualitatively accurate, however the results were not quantitatively accurate because the Iribarne and Thomson model is for ion evaporation from a planar liquid surface. This is physically different from ion evaporation from an ion cluster. Therefore, to produce accurate simulations of ion cluster fragmentation within the acceleration region, models that capture the correct quantitative effect of an external electric field are needed and is an area of future research.

III. Simulation of Ion Plume Evolution

A. Electrospray ion beam properties

The low density of electrospray ion plumes makes the particle-in-cell technique attractive for tracking plume evolution under electrostatic forces. For example, an individual ion beamlet current typically ranges from 100 - 1000 nA. The acceleration region between the emitter tip apex and the extraction grid is 10 - 100 μm .¹⁰ This region is critical to the plume evolution, particularly as fragmentation occurring here will impact the thrust and specific impulse of the ion source. Additionally, resolving ion energies and space-charge potentials in the vicinity of the extractor grid is critical for predicting return currents, which can lead to both erosion and charging. Thus initial PIC simulations of an electrospray ion source will focus on the plume evolution in and just beyond the extraction region, taking into account the fragmentation of solvated species to obtain accurate ion trajectories and energies.

Analytical estimates of expansion at a prescribed divergence angle are useful for creating the simulation architecture. Fig. 5 shows (a) the Laplacian potential distribution in the vicinity of the extraction region and (b) the evolution of plume parameters: ion density (n_i), number of particles in a Debye sphere (N_D), and the ion Debye length (λ_D) on axis for an example 300 nA beamlet expanding at a 30° half-angle. The small simulation domain, coupled with reasonable numbers of particles ($\sim 10^3$) in a Debye-scale volume, allows for individual particle tracking in the PIC algorithm (no macroparticle weighting). Note that in reality, the divergence angle is expected to vary for each species as particles with lower charge-to-mass ratios experience greater deflection.

Fig. 6 shows the divergence angles for EMI-BF4 monomers, dimers, and a typical thruster charge-to-mass ratio,¹⁰ using the paraxial ray approximation for quasi-1D space-charge effects.¹¹ The PIC framework will resolve more accurate trajectories for each particle type in a mixed beam. This mass-dependent spreading has also been observed experimentally with the mean charge-to-mass value decreasing with angle across the beam.¹²

B. Simulation description

The electrospray PIC code under development is called *iePIC* (*ion electrospray Particle in Cell*). Currently, the simulation is carried out in a 3D, Cartesian domain. Particles of various charge-to-mass ratios are

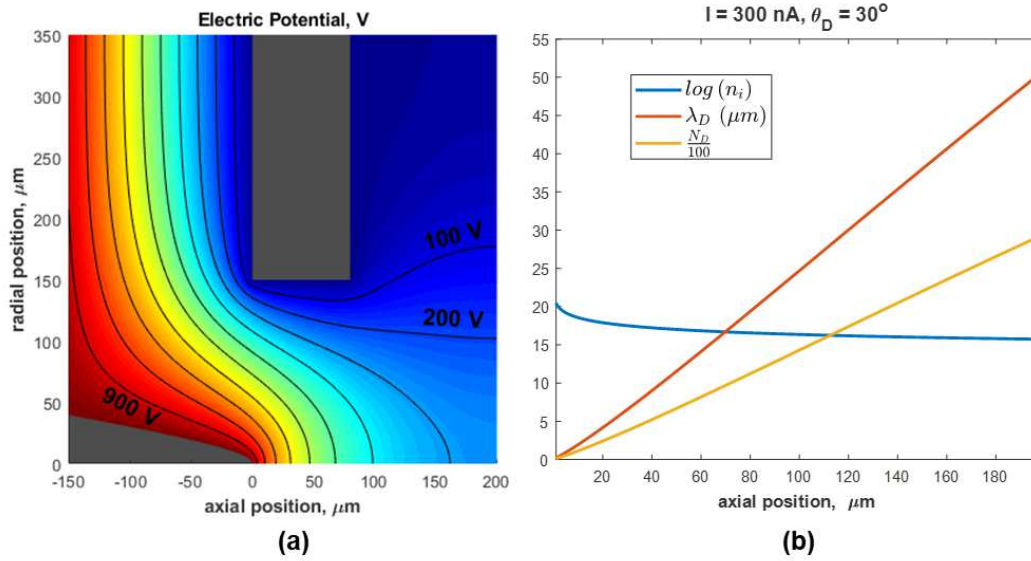


Figure 5: Approximations used to guide simulation development: (a) a Laplacian potential field in the extraction region and (b) predicted evolution of plume parameters on-axis.

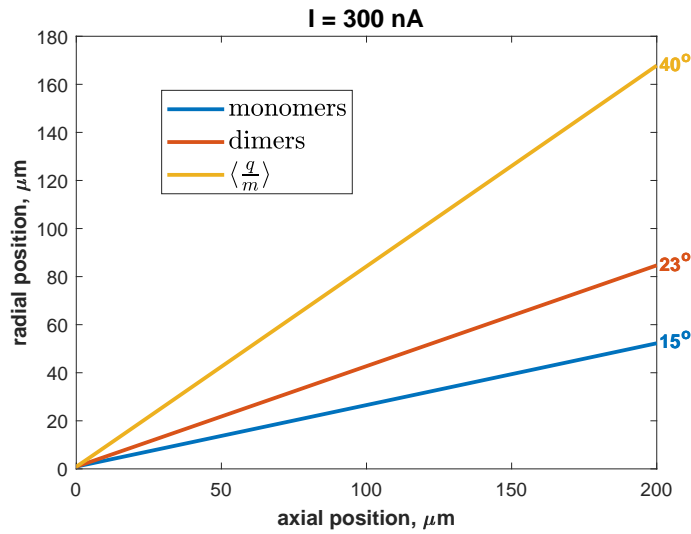


Figure 6: Predicted beam divergence angles for beams of different charge-to-mass ratios: 8.6×10^5 , 3.1×10^5 , 7.2×10^{10} C/kg.

sampled from a distribution function and are injected into the domain at a rate that satisfies the specified beam current. This allows for grouping of particles by ion type with the ability to specify a spread in initial velocity according to the shape of each peak. For the present simulations, only monomers and dimers are injected and the distribution function is simply two delta functions at the appropriate charge-to-mass values.

The region in the immediate vicinity of the emission site is not resolved in this model. Instead, particles are injected within an initial 5 degree angle from the centerline with an initial energy corresponding to the injection potential, V_i .

C. Fragmentation model integration

The fragmentation model is implemented here in the context of a single ion beam. As discussed in Section II.B, solvated ions will decay predictably as a function of time when not acted upon by external forces.

Additionally, the single ion beam framework will make it possible to compare simulated results against previous laboratory research using single emitters. The region of interest is constrained to just beyond the emission site, containing part of the the acceleration region and extending into field-free space. The influence of the accelerating electric field on fragmentation is not yet accounted for and will be the subject of future work.

In building a fragmentation model into the PIC framework, several assumptions are made. First, all ions are modeled as point particles independent of whether they were single ions or solvated clusters (dimers only in this case). This approach allows for internal degrees of freedom of complex ions to be enveloped in the fragmentation model while the PIC algorithm captures the macroscopic electrostatic interactions. During fragmentation, excess internal energy and the geometry of bonding sites between the anion and cation could impart some translational or rotational energy in random directions. However, the energy of solvation ($\mathcal{O} \sim eV$) is much less than the ion kinetic energy ($\mathcal{O} \sim 1000eV$) and thus these effects are neglected. In treating the ions as point particles, both momentum and energy are conserved in this scheme. Fig.7 shows the cluster and product particle momentum and energies before and after the fragmentation event.

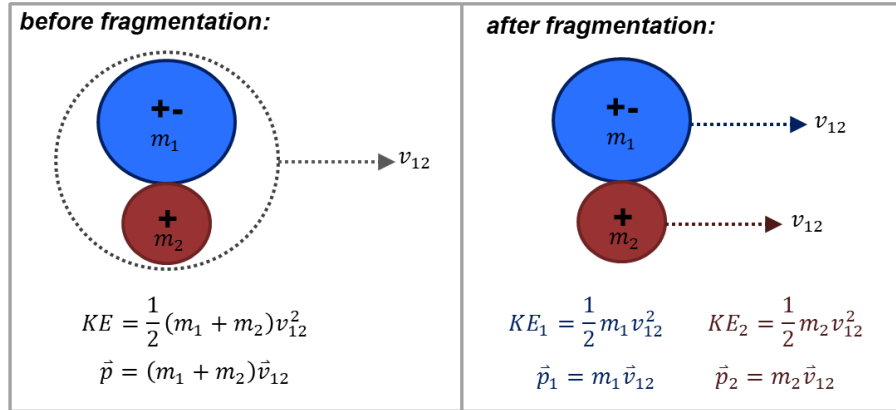


Figure 7: Energy and momentum before and after fragmentation event.

Tracking particle information and the species type (neutral, monomer, or dimer) lent itself to using matrices to store species information. The model employs three species matrices with 3D position and velocity, the dimer matrix having an additional entry for the fragmentation time. Monomer and dimer injection is distributed across each time step to satisfy the prescribed current and species fractions. The dimer is assigned a random fragmentation time sampled from the physically-informed distribution of fragmentation times. Once the particle’s time in the simulation has exceeded its assigned break-up time, it will be destroyed. The dimer’s position and velocity information is transferred to newly created particles in the monomer and neutral matrices. The newly created monomer and neutral are propagated forward in the scheme.

The distribution of fragmentation times is determined such that the dimers will exponentially decay with a characteristic time constant, τ . The normalized distribution function of fragmentation times is thus given by:

$$f(t) = \frac{1}{\tau} e^{-t/\tau} \quad (6)$$

D. Example Results

The evolution of a hypothetical ion plume is simulated to demonstrate the fragmentation algorithm. Simulation parameters are included in Table 1.

In this case, a fragmentation time constant of $9.5 \mu s$ is specified and a drastic change in plume composition occurs the first 1 mm from the emission site. The simulated plume is shown in Fig. 8. Note that the injection angle is particle mass dependent and the ”monomer” population is injected with a larger initial spread in angles than the “dimer” population, hence the apparent smaller divergence angle for dimers and resulting neutrals.

Table 1: PIC Simulation Parameters

Simulated Ion Properties	
I_{beam}	526 nA
$(q/m)_{mon}, f_{0,mon}$	$2.0 \times 10^4, 0.5$
$(q/m)_{dim}, f_{0,dim}$	$3.8 \times 10^4, 0.5$

Domain Properties	
domain size (x,y,z)	$750 \mu m \times 750 \mu m \times 4.8 \text{ mm}$
grid spacing ($\Delta x, \Delta y, \Delta z$)	$1 \times 10^{-5} \text{ m}, 1 \times 10^{-5} \text{ m}, 2 \times 10^{-4} \text{ m}$
injection potential @ $z = 0$	300 V
final potential @ $z = 400 \mu m$	1618 V
time-step (Δt)	$1 \times 10^{-11} \text{ s}$
total time simulated	$3.5 \mu s$

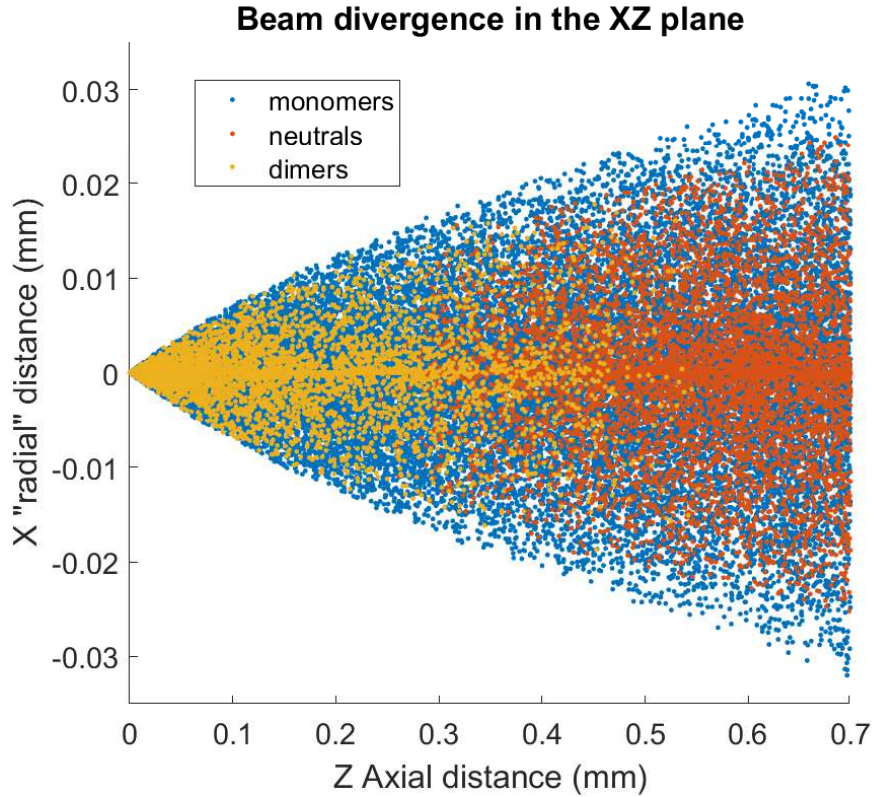


Figure 8: Plot displaying dimers fragmenting in monomers and neutral particles.

E. Conclusions and Future Work

In conclusion, the fragmentation of solvated ions has been experimentally characterized for several ionic liquids and correlated to physical models for an activated process. Solvated species populations are found to decay exponentially with time. Rate constants for dimer to monomer fragmentation in field-free space have been obtained for a range of conditions. This process plays a critical role in the ion plume evolution within the acceleration region and near-field volume.

Initial efforts to incorporate fragmentation into kinetic plume simulations are presented. The model is implemented using an existing, custom-built particle-in-cell (PIC) code developed at MIT capable of tracking ion and droplet emission. Particle trajectories are tracked in 3D in a Cartesian grid. The emission model developed above has been integrated with the PIC code. At the point, the fragmentation rate depends only on the temperature of the ions at emission. Perturbing effects of local electric fields are not yet considered but will be the subject of future work. Currently, each heavy ion emitted in these simulations includes stability information in the form of an assigned fragmentation time that will reproduce exponential decay at an empirically informed rate.

The model developed here will be used to explore the following effects in electrospray ion plumes:

1. Effect of acceleration voltage, current, and fragmentation rate on ion beam expansion
2. Return of fragmented ions - capturing trajectories and impingement rates of low-energy return ions on extraction grid surfaces

Additionally, future work will include extension of the fragmentation algorithm to include the effects of local electric fields, such as in the extraction region, on rate constants. Beyond studies of the immediate thruster extraction and acceleration volume, the end goal is to produce a tool that will provide appropriate descriptions of electrospray plumes to be used as sources in larger, spacecraft-scale simulations.

Acknowledgements

This work was supported by an Early Stage Innovations Grant (No. 80NSSC19K0211) from NASA's Space Technology Research Grants Program. The authors also gratefully acknowledge support from the M. Alemán-Velasco Foundation.

References

- ¹Lozano, P. C., Wardle, B. L., and Moloney, P., “Nanoengineered thrusters for the next giant leap in space exploration,” *MRS Bulletin*, Vol. 40, 2015, pp. 842–849. doi:10.1557/mrs.2015.226.
- ²Araki, S. J., Martin, R. S., Bilyeu, D. L., and Koo, J. W., “SM / MURF : Current Capabilities and Verification as a Replacement of AFRL Plume Simulation Tool COLISEUM,” *52nd AIAA/SAE/ASEE Joint Propulsion Conference, AIAA Propulsion and Energy Forum*, AIAA 2016-4939, Salt Lake City, Utah, 2016. doi:10.2514/6.2016-4939.
- ³Miller, C. E. and Lozano, P. C., “Measurement of the Fragmentation Rates of Solvated Ions in Ion Electro Spray Thrusters,” *52nd AIAA/SAE/ASEE Joint Propulsion Conference, AIAA Propulsion and Energy Forum*, AIAA 2016-4451, Salt Lake City, Utah, 2016.
- ⁴Mier-Hicks, F. and Lozano, P. C., “Spacecraft-Charging Characteristics Induced by the Operation of Electro spray Thrusters,” *Journal of Propulsion and Power*, Vol. 33, No. 2, 2017. doi:10.2514/1.B36292.
- ⁵Legge, R. and Lozano, P. C., “Electro spray propulsion based on emitters microfabricated in porous metals,” *Journal of Propulsion and Power*, Vol. 27, No. 2, 2011, pp. 485–495. doi:https://doi.org/10.2514/1.50037.
- ⁶Lozano, P. C. and Martinez-Sanchez, M., “Efficiency Estimation of EMI-BF₄ Ionic liquid Ion Thrusters,” *41st AIAA/ASME/SAE/ASEE Joint Propulsion Conference & Exhibit, July 10-13, 2005*, Tuscon, AZ, 2005, pp. AIAA-2005-4388.
- ⁷Coles, T. M. and Lozano, P. C., “Investigating Efficiency Losses from Solvated Ion Fragmentation in Electro spray Thruster Beams,” *49th AIAA/ASME/SAE/ASEE Joint Propulsion Conference*, AIAA 2013-4033, San Jose, CA, 2013. doi:10.2514/6.2013-4033.
- ⁸Miller, C. E., *Characterization of Ion Cluster Fragmentation in Ionic Liquid Ion Sources*, Ph.D. thesis, Massachusetts Institute of Technology, 2019.
- ⁹Iribarne, J. and Thomson, B., “On the evaporation of small ions from charged droplets,” *Journal of Chemical Physics*, Vol. 64, 1976, pp. 2287–2294. doi:https://doi.org/10.1063/1.432536.
- ¹⁰Krejci, D., Mier-hicks, F., Thomas, R., Haag, T., and John, N., “Emission Characteristics of Passively Fed Electro spray Microthrusters with Propellant Reservoirs,” *Journal of Spacecraft and Rockets*, Vol. 54, No. 2, 2017, pp. 447–458. doi:10.2514/1.A33531.
- ¹¹Lozano, P., *Studies on the ion-droplet mixed regime in colloid thrusters*, Ph.D. thesis, Massachusetts Institute of Technology, 2003.
- ¹²Perez Martinez, C. S. and Lozano, P. C., “Ion field-evaporation from ionic liquids infusing carbon xerogel microtips,” *Applied Physics Letters*, Vol. 043501, No. 107, 2015, pp. 043501. doi:10.1063/1.4927481.